Accepted 17 April 2017 in *Astrobiology (Special Issue)*

Evaluation of the Tindouf Basin Region in Southern Morocco as an Analog Site for soil Geochemistry on Noachian Mars

Elizabeth A. Oberlin,[1] Mark W. Claire,[2,3,4] and Samuel P. Kounaves[1,5]

[1] Department of Chemistry, Tufts University, Medford, Massachusetts
[2] School of Earth & Environmental Sciences, University of St Andrews, UK
[3] Centre for Exoplanet Science, University of St Andrews, UK
[4] Blue Marble Space Institute of Science, 1001 4th Ave, Seattle, WA USA
[5] Department of Earth Science & Engineering, Imperial College London, UK

Address correspondence to:

Samuel Kounaves
Department of Chemistry
Tufts University
Medford, MA 02155

E-mail: samuel.kounaves@tufts.edu

Running Title: Tindouf Basin Morocco as a Mars Analog

Abstract

Locations on Earth which provide insights into processes that may be occurring or may have occurred throughout martian history are often broadly deemed "Mars analog environments." As no single locale can precisely represent a past or present martian environment, it is important to focus on characterization of terrestrial processes which produce analogous features to those observed in specific regions of Mars, or if possible specific time periods during Martian history. Here, we report on the preservation of ionic species in soil samples collected from the Tindouf region of Morocco and compare them with the McMurdo Dry Valleys of Antarctica, the Atacama Desert in Chile, the Mars meteorite EETA79001, and the in-situ Mars analyses from the Phoenix Wet Chemistry Laboratory (WCL). The Morocco samples show the greatest similarity with those from Victoria Valley (VV), Beacon Valley (BV) and the Atacama, while being consistently depleted compared to University Valley (UV) and enriched compared to Taylor Valley (TV). The NO_3/Cl ratios are most similar to VV and Atacama while the SO_4/Cl ratios are similar to those from BV, VV, and the Atacama. While perchlorate in the Morocco samples are typically lower than other analog sites, conditions in the region are sufficiently arid to retain oxychlorines at detectable levels. Our results suggest that the Tindouf Basin in Morocco can serve as a suitable analog for the soil geochemistry and subsequent aridificiation of the Noachian epoch on Mars.

Kew words or phrases:

Mars analogs, Antarctica, Morocco, oxyanions, perchlorate, nitrate

1. Introduction

The obliquity of Mars has fluctuated throughout the historical martian epochs (Ward, 1973; Touma and Wisdom, 1993; Laskar et al., 2004) causing variations in climate that likely resulted in warmer conditions than are presently observed. Phyllosilicate and evaporite minerals at discrete but globally distributed locations on the surface (Langevin *et al.*, 2005; Mangold *et al.*, 2012; Bibring *et al.*, 2006; Ehlmann *et al.*, 2013; McLennan *et al.*, 2005; Wray *et al.*, 2009; Arvidson *et al.*, 2014; Toon *et al.*, 1980) support the hypothesis that liquid water influenced the martian surface in the past and that the current state of Mars results from the prolonged aridification of the martian environment as aqueous availability decreased with time. The pedogenic processes that occurred during these episodes distributed soluble ionic species that remain as geochemical proxies that can be used to interpret historical climate patterns.

The relative ratios and distribution patterns of salts and their highly soluble anions are commonly examined in order to understand the effects of different degrees of aridity on the geochemical record (Claridge and Campbell, 1977; Cary *et al.*, 1979; Bao *et al.*, 2004; Ewing *et al.*, 2006; Keys and Williams, 1981; Zhu and Yang, 2010; Tamppari *et al.*, 2012; Toner *et al.*, 2013; Jackson *et al.*, 2015). The distribution profiles of accumulated salts in arid soils is a function of their production rates and the duration of aridity. The primary sink for these salts in temperate climates is rainwater flushing of soils to rivers and

groundwater, while in polar regions, mobilization by snowmelt or deliquescence dominates. Thus, comparing environments with similar production mechanisms (generally atmospheric) but differing degrees of aridity can provide insight into the geochemical mechanisms that may have acted during the prolonged aridification of the martian surface. Here, we compare and contrast the ratios of soluble ions in previously suggested "Mars analog" environments with the Tindouf Basin, Morocco, specifically the region of the strewn field of the Mars meteorite, Tissint (Aoudjehane *et al.*, 2012). In particular, we argue that there is no such thing as a unique terrestrial Mars analog locale – rather that Earth contains multiple locations which may serve as analogs for various specific processes at distinct time periods in martian history.

1.1. Introduction to Terrestrial Environments proposed as "Mars Analogs"

1.1.1. McMurdo Dry Valleys, Antarctica. Due to their prolonged state as cold hyperarid deserts, the McMurdo Dry Valleys (MDV) are the most similar of any terrestrial site to the environmental and geological conditions on Mars (both past and present) and thus have been widely used as geochemical and geological martian analogs (Mahaney, 2001; Dickinson and Rosen, 2003; Tamppari *et al.*, 2012; Stroble *et al.*, 2013). While the dry valleys are named as such due to their complete lack of rainfall, except for a few reported instances in coastal MDV they experience precipitation in the form of snowfall, often blown in by the winds.

Most of this snow sublimates in the summer, but there is transfer between snow/soil/permafrost profiles which influences anion profiles (Toner *et al.*, 2013). The different valleys within the MDV can be classified within three distinct climate regions depending on elevation and distance from the coast, which vary in temperature and aqueous availability (Marchant and Head, 2007). Individual valleys can thus be compared in order to understand the effects of the changing martian climate on soil geochemistry. In this way, the relative concentrations of soluble salts between the lower-elevation Taylor Valley (TV), mid-elevation Beacon Valley (BV), through the highest-elevation University Valley (UV) (Tamppari *et al.,* 2012; Stroble *et al.*, 2013; Jackson *et al.,* 2016), can potentially provide insight into the shift in salt accumulation from the martian Noachian to the early Amazonian epochs. These localized environments, which can serve as geochemical analogs throughout the most abrupt climate change periods on Mars, is a uniquely valuable feature of the MDV. However, their remote location and extreme environment hinders accessibility.

1.1.2. Atacama Desert, Chile. The Atacama Desert is the most arid nonpolar desert on Earth. Sedimentological data suggests that it has existed as a stable arid region for the past 150 Ma (Hartley *et al.,* 2005), with evidence of cyclic variations between arid and hyperarid over the past 14 Ma (Jordan *et al.,* 2014). Although the average temperatures in the Atacama of about 16°C (McKay *et al.*, 2003) are much warmer than modern Mars, the hyperarid core of the

123 Atacama features Earth's lowest total precipitation, measured at < 1 mm/yr in the
124 Yungay region (Navarro-González *et al.*, 2003), with even more hyperarid
125 subregions recently identified (Azua-Bustos *et al.*, 2015). The soils found in the
126 Atacama are characterized by high levels of oxyanions such as sulfate ($SO_4^{=}$),
127 nitrate (NO_3^-), and perchlorate (ClO_4^-), as the result of atmospheric or volcanic
128 deposition and input from coastal fog in some regions (Jackson *et al.*, 2005; Bao
129 *et al.*, 2004; Michalski *et al.*, 2004). The relative accessibility of the Atacama has
130 yielded key insights into the geochemistry of hyperarid soils and the processes
131 that drive them (Bao *et al.*, 2004; Ewing *et al.*, 2006; Hartley *et al.*, 2005).
132 1.1.3. Other warm deserts. In order to interpret data from hyperarid soils
133 on Earth in terms of historical martian climates, it is necessary to extend these
134 insights across degrees of aridity. Hyperarid soils on Earth are typically static
135 under relevant timescales. Therefore, it is necessary to characterize environments
136 with similar geologic characteristics but different degrees of aridity for
137 comparison. In this way, we can identify and differentiate the critical processes in
138 these regions and potentially relate soil geochemistry to various martian epochs.
139 The Moroccan desert has previously been proposed as Mars-relevant for
140 operations testing (Ori *et al.*, 2011). Here, we examine the northern Tindouf
141 basin in southeastern Morocco as a region suitable for use as an analog for soil
142 chemistry and aqueous geochemistry across different martian epochs.
143

2. Materials and Methods

2.1. Climate and Geology of Sample Site

The study region is located on the northern edge of the Tindouf basin, in the strewn field from which the Tissint Mars meteorite fragments were recovered. The site is located between the El Aglâb mountains to the north and the Hamada Du Drâa desert to the south, near the El Ga'ïdat plateau (centered within a ~ 6km radius around 29°29'41.29"N, 07°34'50.50"W) (Aoudjehane *et al.*, 2012) (Fig. 1). Broadly speaking, the environment is an inland desert (~220 km inland) free of any evaporitic and sabkha features. The basin, located in the foothills on the southern margin of the Atlas Mountains, feeds into the Draa River (Oued Draa) watershed, which is dry most of the year at this location, consistent with the present day climate of a warm arid desert (Peel *et al.*, 2007). The Tindouf basin contains approximately an 8km thick base layer of Cambrian to Carboniferous marine sediment with approximately 100 m of Pliocene soils deriving from the Atlas Mountains above it (Selley, 1997) and atmospheric input (this study). The study area is near the border with Algeria, and lies entirely within a restricted-accessed zone controlled by the Moroccan military. The area is uninhabited and historically only used for military patrols along well-defined 4x4 tracks, although it has recently experienced substantial foot traffic by Bedouins seeking fragments of the Tissint meteorite.

We divided the study site into two geographically distinct, but physically proximate regions in order to evaluate the influence of the landform variations on the soluble chemistry of the soils. The Ga'ïdat region is located at the southern edge of the site at an average elevation of 400 ± 15 m and consists of a plateau exhibiting little fluvial influence with stable well-developed surface features. The Aglâb region is located at the northern edge of the study site at the base of a mountain with an average elevation of 380 ± 0.5 m. The Aglâb region is characterized by alluvial fans, dry river beds, and variable topography indicative ephemeral streams and other fluvial processes temporarily feeding the River Draa.

2.2. Sampling Procedures

Soil samples were collected from six sites (at 11 pits) in the Aglâb region and from six sites (at 9 pits) in the Ga'ïdat region (Fig. 1). Sampling sites were chosen in flat surfaced areas at local topographic highs, without vegetation or foot tracks, generally with loose to consolidated desert pavement. At each sampling site two shallow pits were dug to a depth of 20 cm; one at a location in which the soil was covered with desert pavement, and a second at a similar location nearby without substantial pavement (Fig. 2). At each site, any surface cobbles were removed, and a "surface" soil/silt sample from 0-5 cm, and a "depth" sample from 15-20 cm were collected and sealed in pre-sterilized Whirl-Pak® sample bags. The sampling depth was chosen as a layer of caliche was encountered in most

areas beginning at 20-30 cm. This was repeated throughout the sampling field to obtain a well-represented coverage of the area.

2.3. Soluble Content Analysis

Soil samples were returned to the laboratory and split into sand (2 mm-75 µm) and fine (< 75 µm) fractions prior to leaching. A 1.0 g portion of both fractions of each sample was leached at a 1:10 soil:water ratio for 1 hour with rocking on a Thermoline Labquake and an aliquot of each leachate was then diluted to a conductivity of 50 µS/cm. The undiluted samples were analyzed for perchlorate (ClO_4^-) and the diluted samples for inorganic anions by ion chromatography using a Dionex ICS2000 under the conditions listed in Table 1. Final concentrations for soil samples were determined by accounting for dilutions and summing the resulting concentrations, weighted by their compositional percentage.

2.4. Comparative Studies

Ionic concentration of samples from this study were compared to soils in five other terrestrial sites of differing aridity and temperature, as well as leachate of the Mars meteorite EETA79001, and the in-situ Mars soil analyses performed by the Wet Chemistry Laboratory (WCL) on board the Mars Phoenix Lander. The soluble ionic distributions in these regions are compared in terms of the differences between preservation potential in these locales, with speculative links to soil geochemistry in different Martian epochs.

205

206 **3. Results**

207 The measured anion content of the soil for the Aglâb and Ga'ïdat sampling
208 regions is shown in Table 2. In both regions the particle size distributions
209 generally consist of a primarily sandy soil with a tendency for fine grained
210 particles to accumulate on the surface. The average particle distributions for
211 depth and surface samples are 90-95 wt% and 75-90 wt% sand particles
212 respectively. A neutral soil pH is observed across the entire study region with an
213 average pH of 7.1 ± 0.5 across all samples and differences between surface and
214 subsurface pH values ranging from 0.3-2%. The electrical conductivity (EC) is
215 less consistent across samples with the RSD values ranging from 130-200% both
216 within and across regions, suggesting a heterogeneous distribution of salts,
217 consistent with variability in our ionic measurements. The EC and pH values for
218 each pit at each site are listed in Table 3. The ionic concentrations are generally
219 higher at depth than at the surface (Table 2). This is especially notable for
220 perchlorate which is below the limit of detection (LOD) of 2.5×10^{-4} mmol/kg in
221 surface samples, but present at up to 2.5×10^{-3} mmol/kg (250 ppb) at 20cm.
222 The relative distribution of oxyanions is used to assess the differences
223 between regions by normalizing against total measured anionic content. This
224 allows for the comparison of the relative distribution patterns between samples
225 without the confounding influence of variable salinity due to differential

preservation and transport. Fig. 3 shows the interquartile range (IQR) for the distribution of anions, normalized against the total measured anionic content. Chloride molar fractions exhibit the greatest variability within sampling regions, and nitrate the smallest. However, nitrate molar fractions exhibit the largest difference between samples sites, with a 72% difference in medians and a 39% difference in the IQR between the Aglâb and Ga'ïdat regions. This is compared to a 48% and 2% difference in median and IQR for chloride and a 2% and 7% difference in median and IQR for sulfate. Surface and depth molar fractions tend to be more consistent between the ions with the median difference of 25%, 10%, and 23% for chloride, sulfate, and nitrate, respectively, while IQR values differed by 20%, 20%, and 15%, respectively. However, differences in IQR for all ions and the difference in median for sulfate, are greater between surface and depth samples, than between sampling regions. Fig. 4 shows the relationship between the concentrations of oxyanions (sulfate, nitrate, and perchlorate) and the chloride for the Moroccan soil samples from this study.

4. Discussion

The relatively similar normalized ionic ratios observed throughout the two sampling regions can be summarized as an overall similarity in terms of salt origin, resulting in a geochemically homogenous area with outlier sample

246 variations due to disparate localized transport processes. This is supported by a
247 greater difference in the more soluble nitrate and chloride ions than sulfate, which
248 would result from the distribution of these highly soluble anions in response to
249 intermittent precipitation events and diurnal condensation.
250 The difference in the concentrations between the surface and the subsurface
251 samples is larger than for the samples from the two regions. This is likely the
252 result of differences in the availability of water to percolate through the soil and
253 ubiquitous surface mixing by aeolian processes. The higher elevation, better
254 developed soil profiles on the Ga'ïdat plateau are generally less susceptible to
255 variation, as evidenced by smaller relative standard deviations in both surface and
256 depth conductivity measurements, likely due to the limited transport processes
257 occurring in the region. On the other hand, the more complex Aglâb region, with
258 its input from aqueous discharge from the nearby mountain and channeling from
259 the surrounding areas in response to the surrounding higher elevation landforms,
260 results in greater variation depending on sampling location. Geomorphological
261 differences aside, the regions can be reasonably considered to be the same in
262 terms of their normalized soluble anion content and are treated as such for further
263 comparison purposes.
264 Perchlorate is one the most soluble naturally-occurring salts, so its presence
265 near the surface implies either an extreme lack of rainfall, or a barrier to vertical
266 diffusion. At the hyper-arid core of the Atacama Desert, where rainfall averages

267 less than 1 mm yr^{-1} (McKay *et al*. 2003), perchlorate is generally leached from
268 soil profiles to at least 50 cm depth (Jackson *et al*. 2015), presumably via
269 exceedingly rare large rainfall events. In the Tindouf, significant rainfall events
270 are typical in the winter months, thus we hypothesize the sporadic perchlorate
271 abundances observed at 15-20 cm depth (from LOD to 2.5×10^{-3} mmol/kg), reflect
272 a localized hydrological control dominated by a vertical barrier at the hardpan
273 caliche. In addition to plant uptake (which does not apply to our sample sites),
274 local geomorphological effects have been shown to cause similar heterogeneity in
275 the Armargosa desert (Andraski *et al.* 2014). There, measured perchlorate
276 deposition fluxes of 3.4 ng cm^{-2} y^{-1} agree with higher-end theoretical predictions
277 of atmospheric perchlorate production from the Atacama desert (Catling *et al.*
278 2010). Assuming these perchlorate production rates apply to the Tindouf, this
279 yields an ~ 10^3 year accumulation time for the 2.5×10^{-3} mmol/kg observed at 20
280 cm depth. We speculate that the caliche layer plays a role in the concentration of
281 soil anions, absorbing moisture from significant rainfall events followed by
282 extreme evaporation, and that only very significant rainfall years would flush out
283 the entire system into the Draa River.
284
285 *4.1. Comparison with Other Proposed Mars Analog Sites*
286 On Earth, nitrate, chloride, and perchlorate in arid and semi-arid soils are
287 known to be primarily of atmospheric origin (Michalski *et al.*, 2004 ; Bao *et al.*,

2004). These ions are also highly water soluble and tend to accumulate in arid and semi-arid environments (Walvoord *et al.*, 2003 ; Jackson *et al.*, 2015). As a result, the ratio of these ions in desert soils can be used in the interpretation of the aqueous processes in these areas. Fig. 5 shows the correlation between the concentrations of oxyanions and chloride concentrations for sulfate, nitrate, and perchlorate, for samples from Morocco (linear fit lines from Fig. 4) compared to samples, from five terrestrial Mars analog sites (Stroble *et al.*, 2013; Tamppari *et al.*, 2012), the Mars meteorite EETA790001 (Kounaves *et al.*, 2014), and the Mars Phoenix WCL analyses (Kounaves *et al.*, 2010).

4.1.1. Atacama. Samples from the Atacama are similar to Morocco in their NO_3/Cl ratios and correlation (Fig. 5a), but differ in their NO_3/ClO_4 ratio (Fig. 7) which is lower than in Morocco. The prolonged hyper-arid conditions in the Atacama compared to Morocco may explain the lower NO_3/ClO_4 ratio observed in the Atacama. Since ClO_4^- is highly soluble and is quickly transported in the presence of water, the prolonged hyper-arid conditions in this region would result in the greater accumulation of ClO_4^-, reducing the NO_3/ClO_4 ratio.

4.1.2. Beacon Valley. The Beacon Valley samples have comparable NO_3/Cl and SO_4/Cl ratios to those observed in the Moroccan samples (Fig. 5b). However, the correlations in both cases demonstrate a greater increase in oxyanion species compared with Cl^- in Beacon Valley. This consistently larger relative increase associated with samples from Beacon Valley indicate a preference for

309 accumulation of oxyanions compared to chloride. This may be due to the higher
310 elevation of Beacon Valley which results in less input of Cl^- from ocean spray
311 and/or a more rapid accumulation of atmospherically derived oxyanion species.
312 Both NO_3^- and ClO_4^- are highly soluble, and their persistence in an environment is
313 indicative of the relative absence of aqueous transport processes. The correlation
314 between NO_3^-, ClO_4^-, and Cl for Beacon Valley falls in the center when compared
315 with the other investigated analog environments (Figs 6 and 7) suggesting that
316 Beacon Valley is an intermediate in terms of the processes driving ionic ratios in
317 these areas.

318 4.1.3. University Valley. The University Valley NO_3/ClO_4 ratios are the
319 most similar to the Morocco samples (Fig. 7), but no other similarities are
320 observed between the data sets. In general, oxyanion ratios and correlations are
321 much larger and steeper in University Valley than other analog sites (Fig. 5c).
322 This is similar to the observations for Beacon Valley, wherein oxyanions
323 accumulate and Cl^- input is minimal, but extended to a more arid environment.

324 4.1.4. Taylor Valley. For Taylor Valley the NO_3^- is well correlated with Cl^-
325 ($R^2 = 0.90$) with a comparable slope to that observed in the Moroccan samples,
326 but is relatively depleted in NO_3^- with respect to Cl^- (Fig. 5d). NO_3^- is similarly
327 well correlated to ClO_4^- ($R^2 = 0.85$) with the shallowest slope observed across all
328 investigated analog sites (Fig. 6), and a two order of magnitude shallower slope
329 than is observed in Morocco. In general, Oxyanion/Cl ratios are lower and

330 oxyanions tend to accumulate less compared to Cl^- in Taylor Valley than in
331 Morocco, with the exception of an enrichment of ClO_4^- relative to Cl^-. This may
332 be the result of an increase in Cl^- compared with NO_3^- in Taylor Valley, as a result
333 of input from ocean water spray.

334 4.1.5. Victoria Valley. The Victoria Valley samples are the most similar of
335 the investigated sites to the Moroccan samples (Fig. 5e). Specifically, comparable
336 ratios are observed between the regions for NO_3/Cl and NO_3/ClO_4 (Fig. 7).
337 However, while NO_3/ClO_4 ratios exhibit a similar correlation between the regions,
338 Victoria Valley has an order of magnitude steeper slope in NO_3/Cl correlation
339 compared with Morocco. The similarity in ratios, but difference in linear fit for
340 Victoria Valley samples is likely related to differences in post-depositional
341 processes such as aqueous transport, which may be more complicated in Victoria
342 Valley compared with Morocco in part due to influences from shallow
343 groundwater and permafrost in this polar region (Levy *et al*, 2011; Marchant and
344 Head, 2007).

345 *4.2. Comparison to Direct Measurements on Mars Samples*

346 Figure 5f shows our results in comparison with two direct measurements of
347 soluble species in martian samples, one from the in-situ WCL analyses of martian
348 soil by the Phoenix Mars Lander (Kounaves *et al.*, 2010) and the other from a
349 carbonate clast in the Mars meteorite EETA79001 (Kounaves *et al.*, 2014). In
350 general, oxyanion species are more concentrated in both the WCL and

EETA79001 samples, while Cl^- is depleted. Of note is the similarity between the relative SO_4^{2-}, NO_3^-, and ClO_4^- values in EETA79001 measurements compared to the Moroccan samples. In general, it is observed that SO_4/Cl, NO_3/Cl and ClO_4/Cl ratios are consistently and similarly higher in EETA79001. Also, of note is the large concentration of ClO_4^- that was measured by the Phoenix WCL compared to EETA79001. This may be indicative of a steady increase in ClO_4^- concentration over time as Cl^- has been shown to be easily oxidized to ClO_4^- on mineral surfaces (Carrier and Kounaves, 2015). A similar tendency is noted in the analog sites wherein ClO_4/Cl ratios increase with increasing aridity. This observation supports the proposition that the higher aridity locales such as University Valley can serve as analogs to more recent martian epochs while the less arid Victoria Valley would serve as an analog to earlier epochs.

4.3. Comparison to The Martian Epochs

A summary of the martian epochs and their proposed corresponding terrestrial analogs are shown in Fig. 8. If we consider the MDV as analogs to the different martian epochs depending on the extent of aqueous influence, we find that it decreases in the order University Valley > Beacon Valley > Victoria Valley > Taylor Valley. In this way, University and Beacon Valley can be roughly considered as analogs to the Amazonian/Hesperian epochs, and Taylor and Victoria Valleys to the Hesparian/Noachian epochs. Due to the greater similarities between the lower elevation Victoria Valley and the Moroccan

samples as compared to the higher elevation University Valley samples, and the likelihood that these similarities are the result of the greater influence of aqueous processes in these regions, we argue that the Moroccan sample locations are potential soil geochemistry analogs to the late Noachian epoch on Mars.

5. Conclusions

The utility of the Tindouf Basin region of southeastern Morocco as a more accessible analog with a similar soil geochemistry to the MDVs is demonstrated by the relative similarity of the distribution of ionic species between the Moroccan samples and other Mars analog sites. In general, samples from this region of Morocco show the greatest similarity with samples from Victoria Valley, Beacon Valley and the Atacama. Moroccan samples are consistently depleted in oxyanion species compared to University Valley and enriched compared with Taylor Valley. Specifically, NO_3/Cl ratios are comparable to many proposed Mars analog sites, with the strongest similarities observed with Victoria Valley and Atacama samples. The SO_4/Cl ratios are likewise similar to those from Beacon Valley, Victoria Valley, and in the Atacama. While perchlorate values in Morocco are typically lower than other analog sites, conditions in the region are sufficiently arid to retain oxychlorines at detectable levels. Processes that may have preferentially increased the perchlorate in other regions could include rapid aqueous accumulation and evaporation of the highly soluble oxychlorines, or the production by direct UV oxidation of chlorine in

chloride-bearing minerals, as has been suggested to occur on Mars (Carrier and Kounaves, 2015). The perchlorate in the Morocco samples is most likely a result of slow accumulation via atmospheric production as occurs over most of the Earth (Catling *et al.,* 2010) though direct UV oxidation cannot be entirely ruled out.

Acknowledgements

We would like to thank Joseph Levy and the anonymous reviewers who helped improve this manuscript. We also thank the Ibn Battuta Centre in particular Gian Gabrile Ori and Kamal Taj-Edine for their assistance with logistics and fieldwork. In addition, we would like to thank the Moroccan military for access as well as Aubrey Zerkle and Gordon Fontaine for their assistance in the field.

Disclosure Statement

No competing financial interests exist.

References

Andraski, B. J., W. A. Jackson, T. L. Welborn, J. K. Böhlke, R. Sevanthi, and D.A. Stonestrom. (2014) Soil, Plant, and Terrain Effects on Natural Perchlorate Distribution in a Desert Landscape. *J. Environ. Qual.* 43:980-994

Aoudjehane, H.C., Avice, G., Barrat, J-A., Boudouma, O., Chen, G., Duke, M.J. M., Franchi, I.A., Gattacceca. J., Grady, M.M., Greenwood, R.C., Herd,

C.D.K., Hewins, R., Jambon, A., Marty, B., Rochette, P., Smith, C.L., Sautter, V., Verchovsky, A., Weber, P., and Zanda, B. (2012) Tissint Martian Meteorite: A Fresh Look at the Interior, Surface, and Atmosphere of Mars. *Science* 338:785-788.

Arvidson, R.E., Squyres, S.W., Bell, J.F., Catalano, J.G., Clark, B.C., Crumpler, L.S., de Souza, P.A., Fairén, A.G., Farrand, W.H., Fox, V.K., Gellert, R., Ghosh, A., Golombek, M.P., Grotzinger, J.P., Guinness, E.A., Herkenhoff, K.E., Jolliff, B.L., Knoll, A.H., Li, R., McLennan, S.M., Ming, D.W., Mittlefehldt, D.W., Moore, J.M., Morris, R.V., Murchie, S.L., Parker ,T.J., Paulsen, G, Rice, J.W., Ruff, S.W., Smith, M.D., and Wolff, M. J. (2014) Ancient Aqueous Environments at Endeavour Crater, Mars. *Science* 343 (6169): 1248097.

Azua-Bustos, A., Caro-Lara, L., and Vicuna, R. (2015) Discovery and Microbial Content of the Driest Site of the Hyperarid Atacama Desert, Chile. *Environ. Microbio.Rep.* 7:388-394.

Bao H., Jenkins K.A., Khachaturyan M., and Díaz G.C. (2004) Different sulfate sources and their post-depositional migration in Atacama soils. *Earth Planet. Sci. Lett.* 224:577-587.

Bao H., and Gu B. (2004) Natural Perchlorate Has a Unique Oxygen Isotope Signature. *Environ. Sci. Technol.*, 38:5073-5077.

433 Bibring J.P., Langevin Y., Mustard J.F., Poulet F., Arvidson R., Gendrin A.,
434 Gondet B., Mangold N., Pinet P., Forget F., Berthe M., Bibring J.P., Gendrin
435 A., Gomez C., Gondet B., Jouglet D., Poulet F., Soufflot A., Vincendon M.,
436 Combes M., Drossart P., Encrenaz T., Fouchet T., Merchiorri R., Belluci G.,
437 Altieri F., Formisano V., Capaccioni F., Cerroni P., Coradini A., Fonti S.,
438 Korablev O., Kottsov V., Ignatiev N., Moroz V., Titov D., Zasova L.,
439 Loiseau D., Mangold N., Pinet P., Doute S., Schmitt B., Sotin C., Hauber E.,
440 Hoffmann H., Jaumann R., Keller U., Arvidson R., Mustard J.F., Duxbury
441 T., Forget F., and Neukum G. (2006) Global mineralogical and aqueous mars
442 history derived from OMEGA/Mars Express data. *Science,* 312:400-4.

443 Carrier B.L., and Kounaves S.P. (2015) The origins of perchlorate in the Martian
444 soil. *Geophys. Res. Lett.* 42:3739-3745.

445 Cary, J.W., Papendick, R.I., and Campbell, G.S. (1979) Water and Salt Movement
446 in Unsaturated Frozen Soil: Principles and Field Observations. *Soil Sci. Soc.*
447 *Am. J.* 43:3-8.

448 Catling D.C., Claire M.W., Zahnle K.J., Quinn R.C., Clark B.C., Hecht M.H., and
449 Kounaves S. (2010) Atmospheric origins of perchlorate on Mars and in the
450 Atacama. *J. Geophys. Res.* 115:E00E11.

451 Claridge, G.G.C., and Campbell, I.B. (1977) The salts in Antarctic soils, their
452 distribution and relationship to soil processes. *Soil Science,* 123:377-384.

453 Dickinson, W.W., and Rosen, M.R. (2003) Antarctic Permafrost: An Analogue
454 for Water and Diagenetic Minerals on Mars. *Geology* 31:199-202.

455 Ehlmann, B.L., Berger, G., Mangold, N., Michalski, J.R., Catling, D.C., Ruff,
456 S.W., Chassefière, E., Niles, P.B., Chevrier, V., and Poulet, F. (2013)
457 Geochemical Consequences of Widespread Clay Mineral Formation in Mars'
458 Ancient Crust. *Space Sci. Rev*. 174:329-364.

459 Ewing, S.A., Sutter, B., Owen, J., Nishiizumi, K., Sharp, W., Cliff, S.S., Perry,
460 K., Dietrich, W., McKay, C.P., and Amundson, R. (2006) A threshold in soil
461 formation at Earth's arid–hyperarid transition. *Geochim. Cosmochim. Acta*,
462 70:5293-5322.

463 Hartley, A.J., Chong, G., Houston, J., and Mather, A.E. (2005) 150 Million Years
464 of Climatic Stability: Evidence from the Atacama Desert, Northern Chile. *J.*
465 *Geol. Soc.* 162:421-424.

466 Jackson, W.A., Davila, A.F., Böhlke, J.K., Sturchio, N.C., Sevanthi, R., Estrada,
467 N., Brundrett, M., Lacelle, D., McKay, C.P., Poghosyan, A., Pollard, W., and
468 Zacny, K. (2016) Deposition, accumulation, and alteration of Cl^-, NO_3^-,
469 ClO_4^- and ClO_3^- salts in a hyper-arid polar environment: Mass balance and
470 isotopic constraints. *Geochim. Cosmochim. Acta* 182:197-215.

471 Jackson, W.A., Böhlke, J. K., Andraski, B. J., Fahlquist, L., Bexfield, L., Eckardt,
472 F.D., Gates, J.B., Davila, A.F., McKay, C.P., Rao, B., Sevanthi, R.,

473 Rajagopalan, S., Estrada, N., Sturchio, N., Hatzinger, P.B., Anderson, T.A.,
474 Orris, G., Betancourt, J., Stonestrom, D., Latorre, C., Li, Y., and Harvey,
475 G.J. (2015) Global patterns and environmental controls of perchlorate and
476 nitrate co-occurrence in arid and semi-arid environments. *Geochim.*
477 *Cosmochim. Acta* 164:502-522.

478 Jackson, W.A., Anderson, T.A., Tian, K., and Tock, R.W. (2005) The Origin of
479 Naturally Occurring Perchlorate : The Role of Atmospheric Processes.
480 *Environ. Sci*. 39:1569-1575.

481 Jordan, T.E., Kirk-Lawlor, N.E., Blanco, P.N., Rech, J.A., and Cosentino, N.J.
482 (2014) Landscape Modification in Response to Repeated Onset of Hyperarid
483 Paleoclimate States since 14 Ma, Atacama Desert, Chile. *Bull. Geol. Soc.*
484 *Am.* 126:1016-1046.

485 Keys J.R., and Williams K. (1981) Origin of crystalline, cold desert salts in the
486 McMurdo region, Antarctica. *Geochim. Cosmochim. Acta* 45:2299-2309.

487 Kounaves, S.P., Hecht, M.H., Kapit, J., Gospodinova, K., DeFlores, L., Quinn,
488 R.C., Boynton, W.V., Clark, B.C., Catling, D.C., Hredzak, P., Ming, D.W.,
489 Moore, Q., Shusterman, J., Stroble, S., West, S.J., and Young, S.M.M.
490 (2010) Wet Chemistry experiments on the 2007 Phoenix Mars Scout Lander
491 mission: Data analysis and results. *J. Geophys. Res.*, 115:E00E10.

492 Kounaves, S.P., Carrier, B.L., O'Neil, G.D., Stroble, S.T., and Claire, M.W.

(2014) Evidence of martian perchlorate, chlorate, and nitrate in Mars meteorite EETA79001: Implications for oxidants and organics. *Icarus*, 229:206-213.

Langevin. Y., Poulet. F., Bibring. J.-P., and Gondet. B. (2005) Sulfates in the North Polar Region of Mars Detected by OMEGA/Mars Express. *Science*, 307:1584-1586.

Laskar, J., A. C. M. Correia, M. Gastineau, F. Joutel, B. Levrard, and P. Robutel (2004), Long term evolution and chaotic diffusion of the insolation quantities of Mars, *Icarus*, 170:343-364.

Levy J.S., Fountain A.G., Gooseff M.N., Welch K.A., and Lyons W.B. (2011) Water tracks and permafrost in Taylor Valley, Antarctica: Extensive and shallow groundwater connectivity in a cold desert ecosystem. *Geological Society of America Bulletin*, 123:2295-2311.

Mahaney, W. (2001) Morphogenesis of Antarctic Paleosols: Martian Analogue. *Icarus*, 154:113-130.

Mangold, N., Carter, J., Poulet, F., Dehouck, E., Ansan, V., and Loizeau, D. (2012) Late Hesperian Aqueous Alteration at Majuro Crater, Mars. *Planet. Space Sci.* 72:18-30.

Marchant, D.R., and Head, J.W. (2007) Antarctic dry valleys: Microclimate zonation, variable geomorphic processes, and implications for assessing

513 climate change on Mars. *Icarus*, 192:187-222.

514 McKay C.P., Friedmann E.I., Gómez-Silva B., Cáceres-Villanueva L., Andersen
515 D.T., and Landheim R. (2003) Temperature and Moisture Conditions for
516 Life in the Extreme Arid Region of the Atacama Desert: Four Years of
517 Observations Including the El Niño of 1997–1998. *Astrobiology*, 3:393-406.

518 McLennan, S.M., Bell, S.F., Calvin, W.M., Christensen, P.R., Clark, B.C., de
519 Souza, P.A., Farmer, J., Farrand, W.H., Fike, D.A., Gellert, R., Ghosh, A.,
520 Glotch, T.D., Grotzinger, J.P., Hahn, B., Herkenhoff, K.E., Hurowitz, J.A.,
521 Johnson, J.R., Johnson, S.S., Jolliff, B., Klingelhofer, G., Knoll, A.H.,
522 Learner, Z., Malin. M.C., McSween, Jr H.Y., Pocock, J., Ruff, S.W.,
523 Soderblom, L.A., Squyres, S.W., Tosca, N.J., Watters, W.A., Wyatt, M., and
524 Yen, A. (2005) Provenance and Diagenesis of the Evaporite-Bearing Burns
525 Formation, Meridiani Planum, Mars. *Earth Planet. Sci. Lett.* 240:95-121.

526 Michalski, G., Böhlke, J.K., and Thiemens, M. (2004) Long term atmospheric
527 deposition as the source of nitrate and other salts in the Atacama Desert,
528 Chile: New evidence from mass-independent oxygen isotopic compositions.
529 *Geochim. Cosmochim. Acta*, 68:4023-4038.

530 Navarro-González, R., Rainey, F.A., Molina, P., Bagaley, D.R., Hollen, B.J., de la
531 Rosa, J., Small, A.M., Quinn, R.C., Grunthaner, F.J., Cáceres, L., Gomez-
532 Silva, B., and McKay, C.P. (2003) Mars-Like Soils in the Atacama Desert,

533 Chile, and the Dry Limit of Microbial Life. *Science*, 302:1018-1021.

534 Ori, G.G., Taj-Eddine, K., and Dell'Arciprete, I. (2011) The Ibn Battuta Centre
535 (Marrakech, Morocco) for Testing Lander Science, Operations and Landing
536 Systems, in *Analogue Sites for Mars Missions: MSL and Beyond*, LPI
537 Contribution No. 161, Abstract 6006.

538 Peel, M.C., Finlayson, B.L., and McMahon, T.A. (2007) Updated World Map of
539 Köppen-Geiger Climate Classification. *Hydrol. Earth Sys. Sci.* 11:1633-44.

540 Selley, R.C. (1997) Chapter 1 The Sedimentary Basins of Northwest Africa, In
541 *Sedimentary Basins of the World Vol. 3: African Basins*, 3-16.

542 Stroble, S.T., McElhoney, K.M., and Kounaves, S.P. (2013) Comparison of the
543 Phoenix Mars Lander WCL soil analyses with Antarctic Dry Valley soils,
544 Mars meteorite EETA79001 sawdust, and a Mars simulant. *Icarus*, 225:933-
545 939.

546 Tamppari, L.K., Anderson, R.M., Archer, P.D., Douglas, S., Kounaves, S.P.,
547 McKay, C.P., Ming, D.W., Moore, Q., Quinn, J.E., Smith, P.H., Stroble, S.,
548 and Zent, A.P. (2012) Effects of extreme cold and aridity on soils and
549 habitability: McMurdo Dry Valleys as an analogue for the Mars Phoenix
550 landing site. *Antarctic Science*, 24:211-228.

551 Toner, J.D., Sletten, R.S., and Prentice, M.L. (2013) Soluble salt accumulations in
552 Taylor Valley, Antarctica: Implications for paleolakes and Ross Sea Ice

553 Sheet dynamics. *J. Geophys. Res. Earth Sur.* 118:198-215.

554 Toon, O.B., Pollack, J.B., Ward, W., Burns, J.A., and Bilski, K. (1980) The
555 Astronomical Theory of Climatic Change on Mars. *Icarus* 44:552-607.

556 Touma, J, and Wisdom, J. (1993) The Chaotic Obliquity of Mars. *Science*
557 259:1294-1297.

558 Walvoord M.A., Phillips F.M., Stonestrom D.A., Evans R.D., Hartsough P.C.,
559 Newman B.D., and Striegl R.G. (2003) A Reservoir of Nitrate Beneath
560 Desert Soils. *Science,* 302:1021-1024.

561 Ward, W. (1973) Large-Scale Variations in the Obliquity of Mars. *Science*
562 181:260-262.

563 Wray, J.J., Noe Dobrea, E.Z., Arvidson, R.E., Wiseman, S.M., Squyres, S.W.,
564 McEwen, A.S., Mustard, J.F., and Murchie, S.L. (2009) Phyllosilicates and
565 sulfates at Endeavour Crater, Meridiani Planum, Mars. *Geophys. Res. Lett.*,
566 36:L21201.

567 Zhu B., and Yang X. (2010) The origin and distribution of soluble salts in the
568 sand seas of northern China. *Geomorphology*, 123:232-242.

569

570 Table 1: Parameters and reagents used for IC analysis of samples. Columns used
571 for all samples were 250mm x 4mm

	Anions	Perchlorate
Dionex Column	AS16	AS18
Eluent	KOH	KOH
Eluent Conc., mM	20	35
Flor Rate, mL/min	1	1.25
Suppressor Current, µS	75	175
Injection Volumer, µL	25	100

572
573

574 Table 2: Measured anion concentration data for the Aglâb and Ga'ïdat region
575 samples

Surface (0-5 cm) Ion Concentration (mmol/kg)						
Region	Sample	Chloride	Sulfate	Nitrate	Chlorate	Perchlorate
Aglâb	1a	3.42 ± 0.123	2.85 ± 0.050	0.57 ± 0.050	0.09 ± 0.010	ND
	1b	5.63 ± 0.052	15.43 ± 0.111	1.06 ± 0.084	0.090 ± 0.008	ND
	2a	2.34 ± 0.045	1.55 ± 0.013	0.38 ± 0.015	0.06 ± 0.004	ND
	2b	2.55 ± 0.008	0.20 ± 0.006	0.26 ± 0.005	0.03 ± 0.002	ND
	3a	0.87 ± 0.023	1.00 ± 0.007	0.45 ± 0.009	0.04 ± 0.002	ND
	3b	0.45 ± 0.005	0.23 ± 0.002	0.34 ± 0.002	0.02 ± 0.001	ND
	4a	44.52 ± 0.395	2.34 ± 0.085	4.69 ± 0.112	0.20 ± 0.025	ND
	4b	282.47 ± 1.687	36.59 ± 0.331	1.45 ± 0.203	ND	ND
	5a	26.51 ± 0.073	11.13 ± 0.049	0.87 ± 0.021	0.11 ± 0.009	ND
	5b	23.97 ± 0.096	11.13 ± 0.024	1.54 ± 0.042	0.12 ± 0.011	ND
	6a	1.68 ± 0.148	1.94 ± 0.145	0.37 ± 0.027	ND	ND
Ga'ïdat	7a	3.86 ± 0.051	0.72 ± 0.012	0.64 ± 0.015	0.06 ± 0.004	ND
	7b	3.58 ± 0.019	0.14 ± 0.002	0.46 ± 0.003	ND	ND
	8a	0.31 ± 0.019	0.32 ± 0.005	0.16 ± 0.007	0.03 ± 0.001	ND
	9a	0.29 ± 0.019	0.22 ± 0.006	0.15 ± 0.008	0.04 ± 0.003	ND
	10a	0.45 ± 0.020	0.28 ± 0.007	0.27 ± 0.007	0.03 ± 0.002	ND
	11a	0.34 ± 0.020	0.30 ± 0.008	0.28 ± 0.007	0.05 ± 0.002	ND
	11b	0.14 ± 0.003	0.13 ± 0.002	0.10 ± 0.002	0.03 ± 0.001	ND
	12a	20.76 ± 0.170	1.97 ± 0.045	0.76 ± 0.043	0.09 ± 0.013	ND
	12b	25.31 ± 0.099	1.96 ± 0.017	0.88 ± 0.023	0.10 ± 0.010	ND
Depth (15-20 cm)Ion Concentration (mmol/kg)						
Region	Sample	Chloride	Sulfate	Nitrate	Chlorate	Perchlorate
Aglâb	1a	102.89 ± 8.882	4.10 ± 1.316	11.96 ± 1.071	ND	4.7E-04 ± 4.80E-05
	1b	14.86 ± 0.128	1.31 ± 0.007	1.17 ± 0.019	0.06 ± 0.006	2.56E-04 ± 4.60E-05
	2a	131.89 ± 2.542	60.01 ± 1.256	11.70 ± 0.389	ND	5.04E-04 ± 4.69E-05
	2b	87.41 ± 1.781	11.97 ± 0.199	13.23 ± 0.175	ND	5.20E-04 ± 4.55E-05
	3a	2.67 ± 0.087	3.79 ± 0.104	1.26 ± 0.032	0.06 ± 0.008	ND
	3b	0.18 ± 0.004	0.11 ± 0.002	0.11 ± 0.003	0.02 ± 0.001	ND
	4a	89.09 ± 62.724	31.00 ± 2.776	27.87 ± 15.474	ND	1.28E-03 ± 4.56E-05
	4b	1460.84 ± 15.221	231.30 ± 1.165	6.33 ± 0.818	ND	ND
	5a	151.76 ± 4.374	55.72 ± 1.091	8.80 ± 0.442	ND	4.38E-04 ± 1.23E-04
	5b	55.86 ± 1.682	37.58 ± 1.562	3.26 ± 0.157	ND	ND
	6a	1.49 ± 0.081	6.70 ± 0.032	0.13 ± 0.025	ND	ND
Ga'ïdat	7a	15.03 ± 0.384	1.27 ± 0.106	4.57 ± 0.260	ND	2.50E-03 ± 2.02E-05
	7b	165.20 ± 1.366	24.68 ± 0.071	24.65 ± 0.094	ND	4.25E-04 ± 2.12E-05
	8a	3.17 ± 0.081	3.34 ± 0.039	1.60 ± 0.034	0.07 ± 0.011	ND
	9a	21.75 ± 0.583	63.88 ± 0.440	7.79 ± 0.241	ND	ND
	10a	11.08 ± 0.206	14.73 ± 0.316	6.14 ± 0.123	ND	2.72E-04 ± 2.02E-05
	11a	2.71 ± 0.064	3.66 ± 0.042	1.49 ± 0.026	0.01 ± 4.83E-04	ND
	11b	0.92 ± 0.006	1.03 ± 0.005	0.57 ± 0.003	0.03 ± 0.001	ND
	12a	980.52 ± 40.339	163.47 ± 10.130	121.07 ± 7.713	0.56 ± 0.148	1.57E-03 ± 3.35E-05
	12b	242.80 ± 12.422	12.85 ± 0.628	21.82 ± 1.211	ND	9.01E-04 ± 4.94E-05

576

Table 3: pH, conductivity, and grain size distribution data for the Aglâb and Ga'ïdat region samples

Region	Sample	pH		EC (µS/cm)		2000-75 µm (wt %)		< 75 µm (wt %)	
		0-5 cm	15-20 cm	0-5 cm	15-20 cm	0-5 cm	15-20 cm	0-5 cm	15-20 cm
Aglâb samples	1a	6.96	6.87	146.51	1373.16	82.7%	95.0%	17.3%	5.0%
	1b	7.64	7.68	480.07	243.56	87.4%	90.0%	12.6%	10.0%
	2a	7.56	6.92	123.40	2487.04	74.8%	96.0%	25.2%	4.0%
	2b	7.87	7.08	119.42	1374.29	86.9%	90.7%	13.1%	9.3%
	3a	6.86	6.81	105.14	209.37	79.9%	91.2%	20.1%	8.8%
	3b	7.13	7.24	57.23	45.56	93.0%	94.0%	7.0%	6.0%
	4a	7.34	6.63	594.49	7702.38	87.9%	92.0%	12.1%	8.0%
	4b	8.04	7.12	4033.56	17484.78	92.2%	92.3%	7.8%	7.7%
	5a	7.01	6.48	126.12	3178.29	84.6%	94.1%	15.4%	5.9%
	5b	6.24	6.39	613.24	1418.46	81.6%	92.5%	18.4%	7.5%
	6a	6.91	9.06	110.68	267.70	78.5%	88.4%	21.5%	11.6%
	average	7.23 ± 0.52	7.12 ± 0.74	591.8 ± 1160.6	3253.1 ± 5204.6	84.5% ± 5.7%	92.4% ± 2.3%	15.5% ± 5.7%	7.6% ± 2.3%
Ga'ïdat samples	7a	6.91	7.10	70.01	205.79	82.8%	95.1%	17.2%	4.9%
	7b	7.25	6.90	98.16	955.86	87.7%	93.2%	12.3%	6.8%
	8a	6.91	7.17	1077.74	346.78	73.9%	90.2%	26.1%	9.8%
	9a	7.46	7.12	75.53	534.32	77.5%	89.4%	22.5%	10.6%
	10a	7.45	7.33	59.55	199.91	74.2%	90.1%	25.8%	9.9%
	11a	7.63	6.84	418.21	3330.37	84.4%	91.9%	15.6%	8.1%
	11b	7.11	7.11	68.08	97.41	83.6%	85.3%	16.4%	14.7%
	12a	6.44	6.34	540.50	2783.86	81.7%	89.2%	18.3%	10.8%
	12b	7.72	6.87	508.47	3442.72	87.0%	92.2%	13.0%	7.8%
	average	7.21 ± 0.41	6.97 ± 0.29	324.0 ± 348.3	1321.9 ± 1430.8	81.4% ± 4.8%	90.7% ± 2.8%	18.6% ± 5.1%	9.3% ± 2.8%

583 **Figure Legends**

584 Figure 1: Sampling locations in the Tindouf Basin region in southeastern
585 Morocco.

586 Figure 2: Image showing the two locations where pits were dug, the first at a
587 location in which the soil was covered with desert pavement (foreground) and a
588 second one nearby without substantial pavement (upper left corner).

589 Figure 3: The interquartile range (IQR), normalized against the total measured
590 anionic content, for the distribution of (a) Nitrate, (b) Sulfate, and (c) Chloride

591 Figure 4: Logarithmic plot showing the linear correlation (line) of the
592 concentrations of sulfate (blue), nitrate (red), and perchlorate (green), with the
593 concentration of chloride for the Moroccan soil samples from this study.

594 Figure 5: Logarithmic plots of oxyanion vs chloride concentrations for sulfate
595 (blue), nitrate (red), and perchlorate (green), for samples from Morocco (linear fit
596 lines from Fig. 3) compared to samples, from (a) Atacama (b) Beacon Valley (c)
597 University Valley (d) Taylor Valley (e) Victoria Valley (f) Mars, (symbols).

598 Figure 6: Correlation of nitrate and perchlorate concentrations for all the Mars
599 analog sites in this study.

600 Figure 7: Correlation of NO_3/ClO_4 and Cl/NO_3 average ratios for each martian
601 analog site.

602 Figure 8: Proposed martian epochs most relevant to “Mars analog sites” , based
603 on soil anion geochemistry and aridity .
604

Figure 1

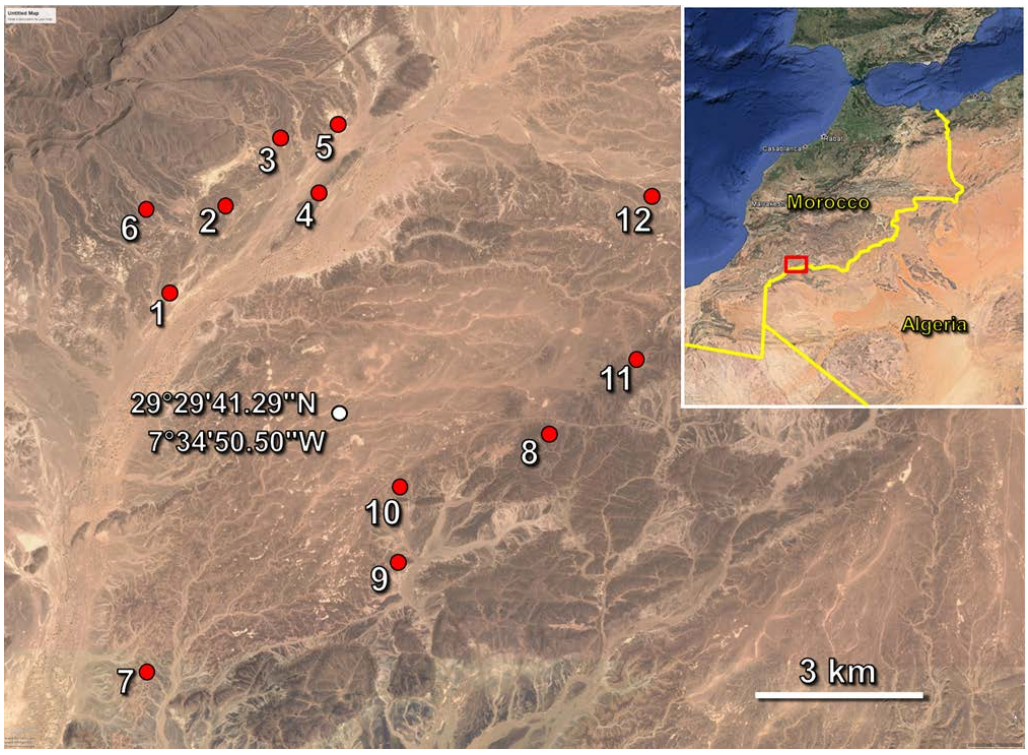
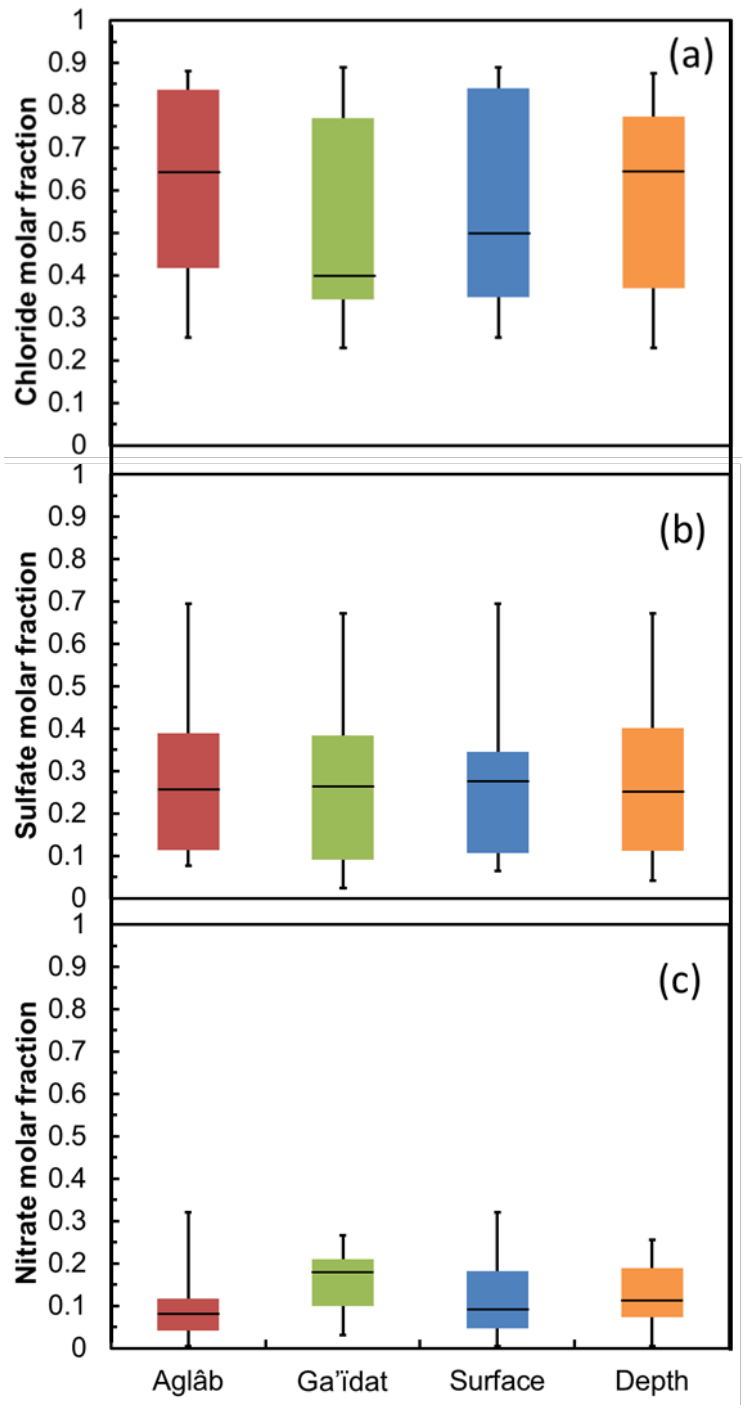


Figure 2



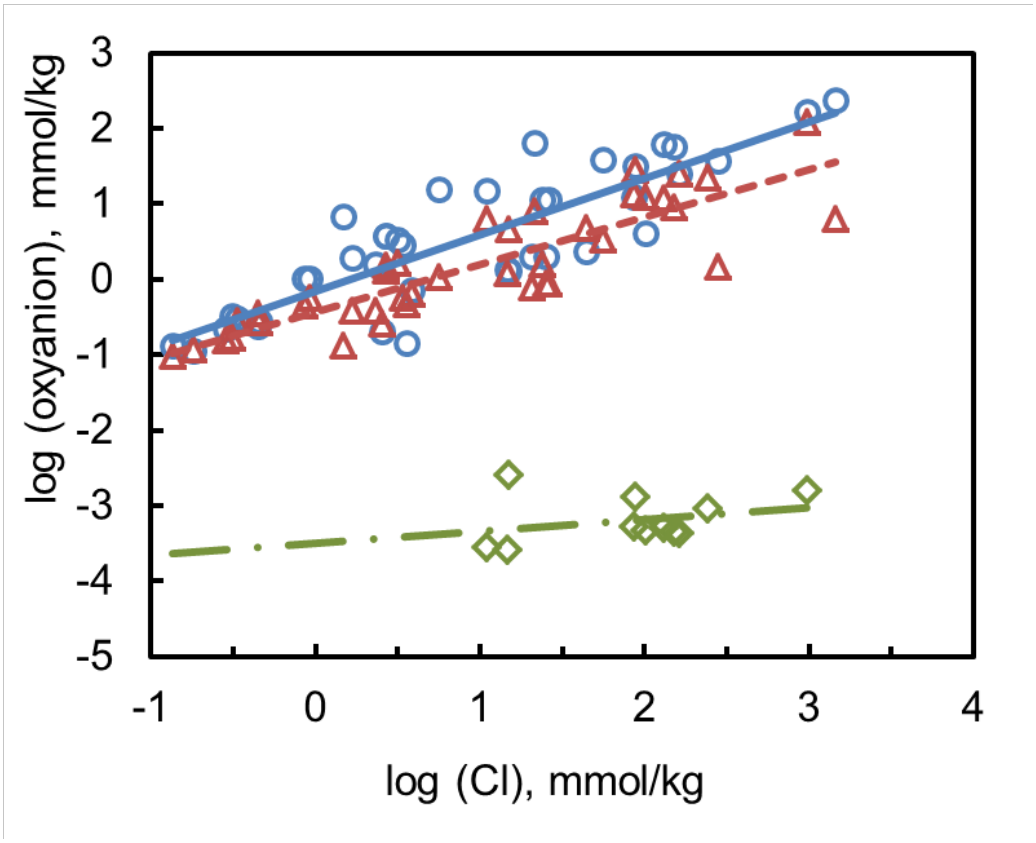
609 **Figure 3**



610

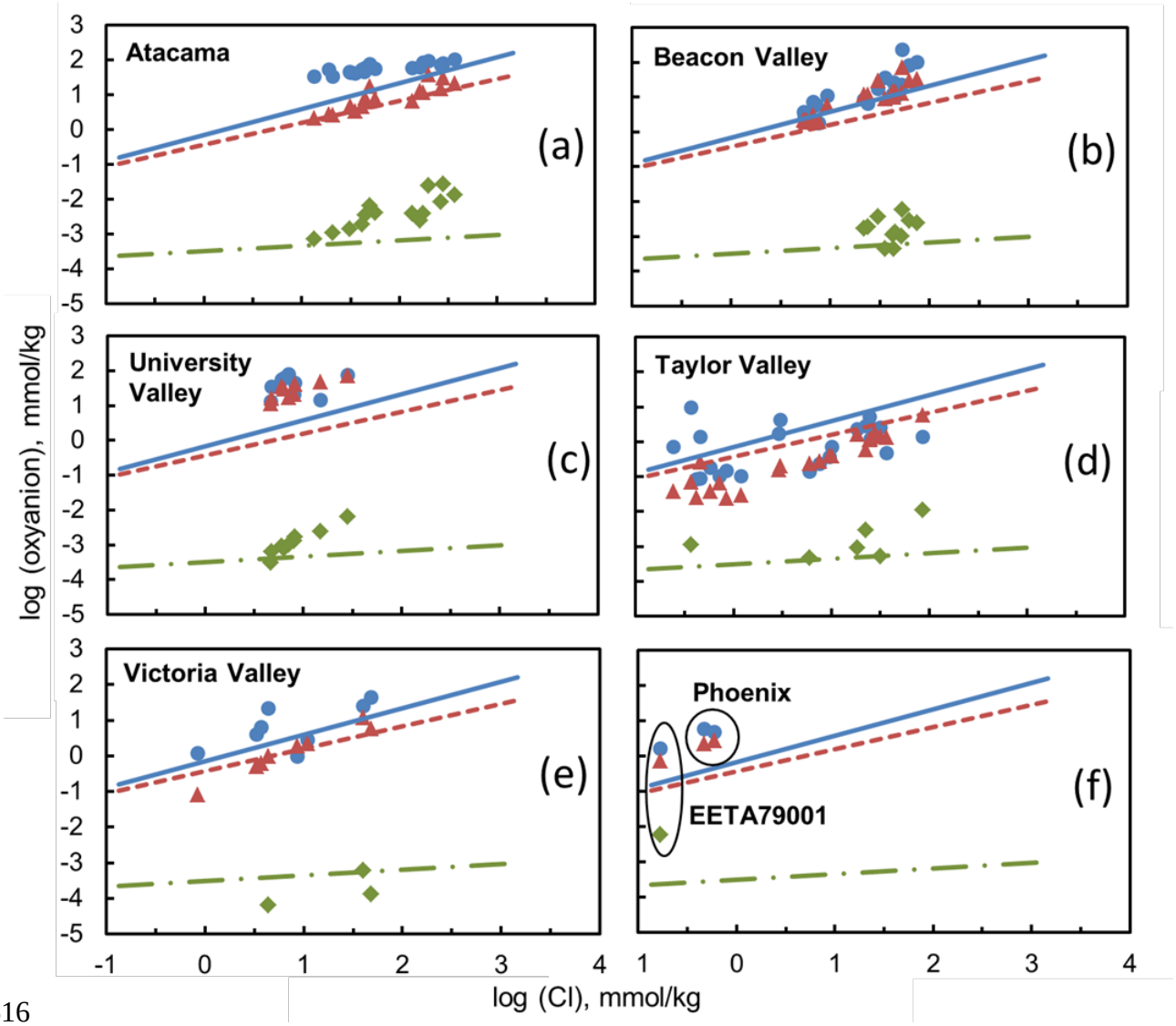
611

612 **Figure 4**



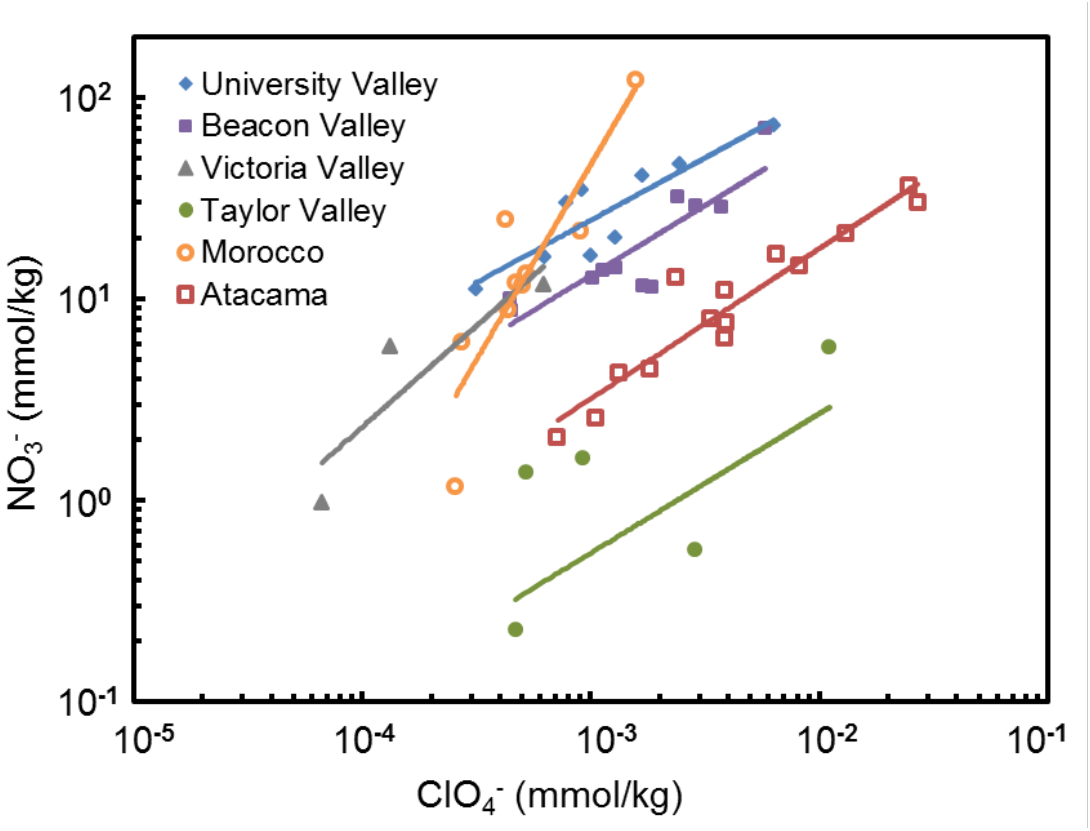
613
614

615 **Figure 5**



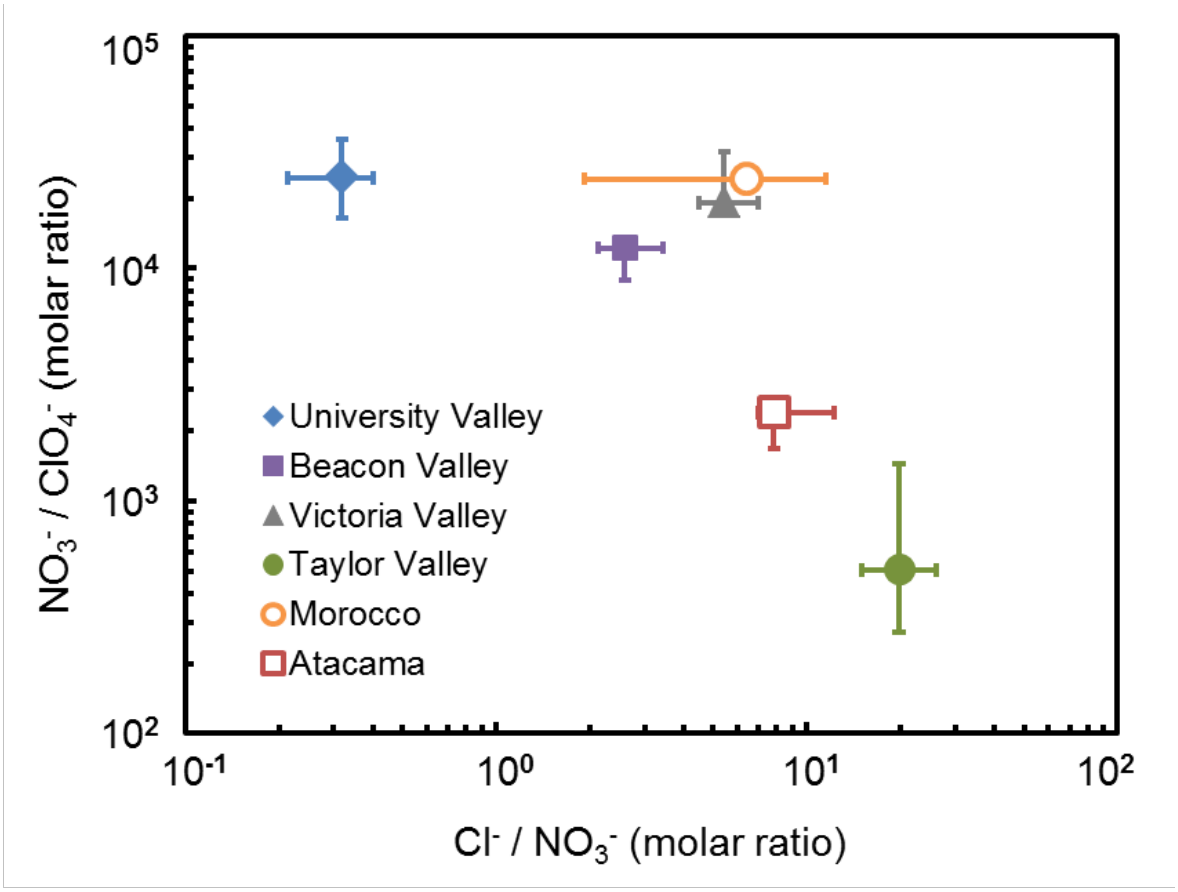
616
617

618 **Figure 6**



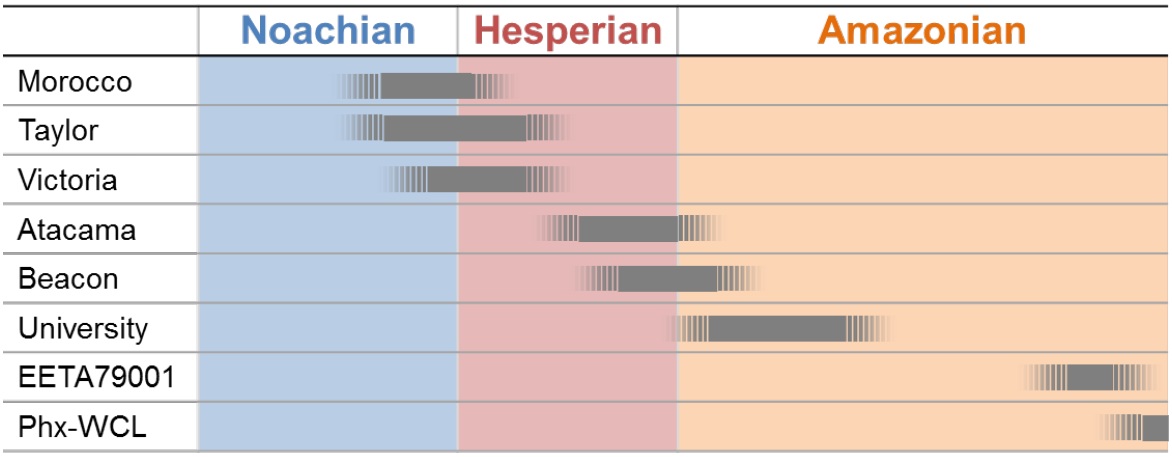
619
620

621 **Figure 7**



622
623

624
625 **Figure 8**



626
627